Quark matter in a parallel electric and magnetic field background: Chiral phase transition and equilibration of chiral density

M. Ruggieri[1,*] and G. X. Peng[1,2,†]

[1]*College of Physics, University of Chinese Academy of Sciences, Yuquanlu 19A, Beijing 100049, China*
[2]*Theoretical Physics Center for Science Facilities, Institute of High Energy Physics, Beijing 100049, China*

(Received 2 March 2016; published 20 May 2016)

In this article, we study spontaneous chiral symmetry breaking for quark matter in the background of static and homogeneous parallel electric field $\boldsymbol{E}$ and magnetic field $\boldsymbol{B}$. We use a Nambu-Jona-Lasinio model with a local kernel interaction to compute the relevant quantities to describe chiral symmetry breaking at a finite temperature for a wide range of E and B. We study the effect of this background on the inverse catalysis of chiral symmetry breaking for E and B of the same order of magnitude. We then focus on the effect of the equilibration of chiral density n_5, produced dynamically by an axial anomaly on the critical temperature. The equilibration of n_5, a consequence of chirality-flipping processes in the thermal bath, allows for the introduction of the chiral chemical potential μ_5, which is computed self-consistently as a function of the temperature and field strength by coupling the number equation to the gap equation and solving the two within an expansion in E/T^2, B/T^2, and μ_5^2/T^2. We find that even if chirality is produced and equilibrates within a relaxation time τ_M, it does not change drastically the thermodynamics, with particular reference to the inverse catalysis induced by the external fields, as long as the average μ_5 at equilibrium is not too large.

DOI: 10.1103/PhysRevD.93.094021

I. INTRODUCTION

There has recently been an increasing interest for the study of systems with a finite chiral density, namely, $n_5 \equiv n_R - n_L \neq 0$. Such a chirality imbalance can be obtained dynamically because of the Adler-Bell-Jackiw anomaly [1,2] when fermions interact with nontrivial gauge field configurations characterized by a topological index named the winding number, Q_W. In the context of quantum chromodynamics (QCD), such nontrivial gauge field configurations at a finite temperature in Minkowski space are named sphalerons, whose production rate has been estimated to be quite large [3,4]. The large number of sphaleron transitions in a high temperature suggests the possibility that net chirality might be abundant (locally) in the quark-gluon plasma phase of QCD; when one couples this thermal QCD bath with an external strong magnetic field $\boldsymbol{B}$, produced in the early stages of heavy ion collisions, the coexistence of $n_5 \neq 0$ and $\boldsymbol{B} \neq 0$ might lead to a charge separation phenomenon named the chiral magnetic effect (CME) [5,6], which has been observed experimentally in zirconium pentatelluride [7]. Beside CME, other interesting effects related to the anomaly and chiral imbalance can be found in Refs. [8–22].

In order to describe systems with finite chirality in thermodynamical equilibrium, it is customary to introduce a chiral chemical potential μ_5, conjugated to the n_5 [23–36]. The chiral chemical potential describes a system in which chiral density is in thermodynamical equilibrium; however, because of the anomaly as well as of chirality-changing processes due to a finite quark condensate, n_5 is not a strictly conserved quantity—hence, the meaning of μ_5 is not so clear; however, naming τ_M the typical time scale in which chirality-changing processes take place, one might assume that $\mu_5 \neq 0$ describes a system in thermodynamical equilibrium with a fixed value of n_5 on a time scale much larger than τ_M, the latter representing the time scale needed for n_5 to equilibrate.

In this article, we study the chiral phase transition and chiral density production in the context of quark matter in background static and homogeneous parallel electric, $\boldsymbol{E}$, and magnetic, $\boldsymbol{B}$, fields. One of our goals is to investigate the effect of the background fields on chiral symmetry breaking at zero temperature and on the critical temperature for chiral symmetry restoration, T_c. This part of the study embraces previous studies about chiral symmetry breaking or restoration in the background of external fields [37–46], completing them by adding the computation of the critical temperature versus the strength of E and B. We find that the effect of the electric field is to lower the critical temperature, in agreement with the scenario of inverse catalysis depicted in Refs. [38,39,47], where, however, only the zero temperature case has been considered; the inverse catalysis scenario does not change considerably when the magnetic field is added, as long as the magnetic field is not very large compared to the electric one. This finding is in agreement with a previous study at zero temperature [37], where the role of the second electromagnetic invariant, $\boldsymbol{E} \cdot \boldsymbol{B}$, has

*marco.ruggieri@ucas.ac.cn
†gxpeng@ucas.ac.cn

been recognized as an inhibitor of chiral symmetry breaking.

We are also interested to study the effect of chiral density on the thermodynamics of the system. The model studied here has the advantage that a chiral density is obtained dynamically without the need to introduce, *a priori*, a chiral chemical potential. As a matter of fact, chirality can be produced by combining $\boldsymbol{E}$, which produces pairs via the Schwinger mechanism, and $\boldsymbol{B}$, which aligns particle spin along its direction. The mechanism producing chirality is very simple: We assume for the sake of simplicity a very large $\boldsymbol{B}$, so that only the lowest Landau level (LLL) is occupied; moreover, we assume the system to be made only of one flavor of quarks, namely, u quarks, and we focus on a single $u\bar{u}$ created by the Schwinger effect. The u quark must have its spin aligned along $\boldsymbol{B}$, because it sits in the LLL, and its momentum will be initially rather parallel or antiparallel to $\boldsymbol{B}$, so the initial helicity can be either positive or negative. On the other hand, the effect of $\boldsymbol{E}\|\boldsymbol{B}$ is to accelerate u along the direction of $\boldsymbol{B}$ so after some time the u quark will have positive helicity. An analogous discussion can be done for the $\bar{u}$. Therefore, as a consequence of the Schwinger effect, LLL, and $\boldsymbol{E}\|\boldsymbol{B}$ each time a pair is created, there is an increase of a factor of 2 of the net chiral density of the system.

The dynamical evolution of n_5 produced by this mechanism can be computed explicitly [48], and it has been shown to be the one expected from the Adler-Bell-Jackiw anomaly: This is not surprising, because $\boldsymbol{E}\cdot\boldsymbol{B}\neq 0$, meaning that the axial current is not conserved at the quantum level and n_5 should evolve according to the anomaly equation. If n_5 evolution was governed only by the anomaly, however, there would be no chance for reaching a thermodynamical equilibrium, because n_5 would grow indefinitely (assuming the fields as external fields and neglecting any backreaction from the fermion currents). But in the thermal bath there are also chirality-flipping processes related to the existence of the chiral condensate as well as of the finite current quark mass: We introduce a relaxation time for chirality, namely, τ_M, giving the time scale necessary for the equilibration of n_5. Then it is possible to show that, for times $t\gg\tau_M$, the chiral density equilibrates to $n_5^{\rm eq}$, the actual value depending on the quark electric charge, field magnitude, and temperature.

Because n_5 equilibrates, it is possible to introduce the chiral chemical potential μ_5, conjugated to $n_5^{\rm eq}$ at equilibrium. Differently from previous calculations with chirality imbalance, in the present study we compute the value of μ_5 self-consistently by coupling the gap equation to the number equation, even if we limit ourselves to the approximation of small fields and small μ_5, namely, working at the leading order in μ_5/T, E/T^2, and B/T^2. As a consequence, μ_5 will depend on the temperature as well as on external fields and on the relaxation time. We focus on the effects of the external fields on the chiral phase transition, with an emphasis on the role of chirality production in the critical region. Because of the small field approximation involved in the solution of the gap as well as the number equations, we are aware that our picture about thermodynamics might change in the case of large fields.

In this study, we compute the effect of the dynamically produced n_5 on T_c. As mentioned above, the $\boldsymbol{E}\cdot\boldsymbol{B}$ term tends to lower the critical temperature; on the other hand, the chiral chemical potential has the effect to increase T_c [23,24,29–34]. Therefore, it is interesting to compute the response of T_c to the simultaneous presence of μ_5 and fields, to check if the inverse catalysis scenario obtained at $\mu_5=0$ still persists at $\mu_5\neq 0$. We can anticipate our results, namely, that chiral density does not affect drastically the thermodynamics at the phase transition, confirming the inverse catalysis induced by the fields, as long as the average chiral chemical potential in the crossover region turns out to be small with respect to the temperature. In Sec. V, we present a detailed study of this effect, showing concrete numbers and among other things how changing the field strengths and/or the relaxation time magnitude affects the inverse catalysis. In fact, we have found and report about situations in which we can measure a net effect of the chiral chemical potential on the constituent quark mass and on the critical temperature, even if we take these results with a grain of salt, as the value of μ_5 at equilibrium turns out to be of the order of the critical temperature, hence potentially validating our quantitative predictions.

The relaxation time for chirality adds the greatest theoretical uncertainty to our calculations: In the absence of a specific calculation of τ_M, it is possible to give only a rough estimate based on dimensional analysis as well as on physical reasons; we chose $\tau_M\propto 1/M_q$, where M_q is the constituent quark mass which is computed self-consistently within the model: It depends on the temperature and fields, and by construction it brings information about the chiral condensate at zero as well as finite temperature. Because of this uncertainty on τ_M, we feel it is not so important, in this explorative study, to present the most complete calculation possible taking into account the full propagators with the full μ_5 dependence: We suspect in fact that, even within the most accurate calculation possible, the new effects of the chiral density on the phase transition might be canceled by changing τ_M, which still would remain unknown. We therefore prefer to limit ourselves to a simple weak field and small μ_5 approximation to explore the effects the chiral density will have on the phase diagram, leaving a more complete calculation to a future study.

The plan of the article is as follows. In Sec. II, we briefly review the model we use for our calculations. In Sec. III, we present a few selected results at zero temperature which show the interplay between the electric and magnetic fields on chiral symmetry breaking. In Sec. IV, we discuss some result at a finite temperature, with an emphasis on the chiral phase transition without taking into account chirality

production. In Sec. V, we compute the chirality at equilibrium and the related chiral chemical potential and study the effect of this chirality on the critical temperature. Finally, in Sec. VI, we draw our conclusions.

II. THE MODEL

In this article, we are interested to study quark matter in a background of an electric-magnetic fluc tube made of parallel electric, $\boldsymbol{E}$, and magnetic, $\boldsymbol{B}$, fields. We assume the fields are constant in time and homogeneous in space; moreover, we assume they develop along the z direction. In this section, we describe the model we use for our calculations. More specifically, we use a Nambu-Jona-Lasinio (NJL) model [49,50] (see [51,52] for reviews) with a local interaction kernel, in which we introduce the coupling of quarks with the external electric and magnetic fields. The setup of the gap equation has been presented in great detail in Ref. [47], which we follow; therefore, we will skip all the technical details and report here only the few equations we need to specify the interactions used in the calculations. The Euclidean Lagrangian density is given by

$$\mathcal{L} = \bar{\psi}(i\not{D} - m_0)\psi + G[(\bar{\psi}\psi)^2 + (\bar{\psi} i\gamma_5 \boldsymbol{\tau}\psi)^2], \quad (1)$$

with ψ being a quark field with Dirac, color, and flavor indices, m_0 is the current quark mass, and $\boldsymbol{\tau}$ denotes a vector of Pauli matrices on flavor space. The interaction with the background fields is embedded in the covariant derivative $\not{D} = (\partial_\mu - iA_\mu\hat{q})\gamma_\mu$, where γ_μ denotes the set of Euclidean Dirac matrices and $\hat{q}$ is the quark electric charge matrix in flavor space. In this work, we use the gauge $A_\mu = (iEz, 0, -Bx, 0)$.

Introducing the auxiliary field $\sigma = -2G\bar{\psi}\psi$ and using a mean field approximation, the thermodynamic potential can be written as

$$\Omega = \frac{(M_q - m_0)^2}{4G} - \frac{1}{\beta V}\mathrm{Tr}\log\beta(i\not{D} - M_q), \quad (2)$$

where the constituent quark mass is $M_q = m_0 - 2G\langle\bar{\psi}\psi\rangle$, $\beta = 1/T$, and βV corresponds to the Euclidean quantization volume. The constituent quark mass differs from m_0 because of spontaneous chiral symmetry breaking, the latter being related to a nonvanishing chiral condensate, $\langle\bar{\psi}\psi\rangle \neq 0$. Even if it would be more appropriate to discuss chiral symmetry restoration via the quark condensate, because it has its counterpart in QCD, in this article we will refer to M_q for simplicity, keeping in mind that whenever we discuss the chiral phase transition in terms of M_q the decrease of the latter is related to the decreasing chiral condensate.

In this model, the main task is to compute self-consistently M_q at a finite temperature and in the presence of the external fields. This is achieved by requiring the physical value of M_q to minimize the thermodynamic potential, and this in turn implies that M_q satisfies the gap equation, $\partial\Omega/\partial M_q = 0$, namely,

$$\frac{M_q - m_0}{2G} - \frac{1}{\beta V}\mathrm{Tr}\mathcal{S}(x, x') = 0, \quad (3)$$

where $\mathcal{S}(x, x')$ corresponds to the full fermion propagator in the electric and magnetic field background. The computation of the propagator has been already given in detail in Ref. [47]; therefore, here we merely quote the final result for the gap equation, that is,

$$\frac{M_q - m_0}{2G} = M_q\frac{N_c}{4\pi^2}\sum_f\int_0^\infty\frac{ds}{s^2}e^{-M_q^2 s}\mathcal{F}(s) + M_q\frac{N_c N_f}{4\pi^2}\int_{1/\Lambda^2}^\infty\frac{ds}{s^2}e^{-M_q^2 s}, \quad (4)$$

where we have introduced the functions

$$\mathcal{F}(s) = \theta_3\left(\frac{\pi}{2}, e^{-|\mathcal{A}|}\right)\frac{q_f eBs}{\tanh(q_f eBs)}\frac{q_f eEs}{\tan(q_f eEs)} - 1 \quad (5)$$

with $\theta_3(x, z)$ being the third elliptic theta function, and

$$\mathcal{A}(s) = \frac{q_f eE}{4T^2\tan(q_f eEs)}. \quad (6)$$

In Eq. (4), we have added and subtracted the zero field contribution on the right-hand side which is the only one to diverge, and we have regularized it by cutting the integration at $s = 1/\Lambda^2$; on the other hand, we have not added a cutoff on the field-dependent part as it is not divergent. For the parameter choice we use the standard parameter set for a proper time regularization [51], namely, $\Lambda = 1086$ MeV and $G = 3.78/\Lambda^2$.

The presence of the $1/\tan(q_f eEs)$ in Eq. (5) implies the existence of an infinite set of poles on the integration in s in Eq. (4); these poles appear in Ω as well. Following the original treatment by Schwinger [53], these poles are moved to the complex plane by adding a small imaginary part which allows one to perform the s integration in the principal value; this leads to an imaginary part of the free energy, which is a sign of the vacuum instability induced by the static electric field [53,54] and leads to particle pair creation. We will consider the effect of this vacuum instability in Sec. V, because it can be directly connected to chiral density production in the case of parallel $\boldsymbol{E}$ and $\boldsymbol{B}$.

III. RESULTS AT ZERO TEMPERATURE

In this section, we present a few results at zero temperature. In Fig. 1, we plot the constituent quark mass as a function of the external field strength at $T = 0$ for several cases: The maroon dot-dashed line corresponds to the case of a pure magnetic field; the green dashed line corresponds

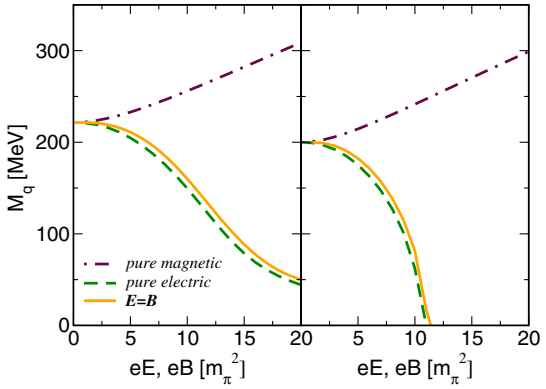

FIG. 1. Dynamical quark mass with the electric and/or magnetic field strength at zero temperature. The maroon dot-dashed line corresponds to the case of a pure magnetic field; the green dashed line corresponds to a pure electric field; and, finally, the solid orange line corresponds to the case $E = B$. The left panel corresponds to $m_0 = 5.49$ MeV, while the right panel corresponds to $m_0 = 0$.

to a pure electric field; and, finally, the solid orange line corresponds to the case $E = B$. The left panel corresponds to $m_0 = 5.49$ MeV, which is the value of the current quark mass necessary to have $m_\pi = 139$ MeV; the right panel corresponds to the chiral limit $m_0 = 0$. For the case of a pure magnetic field, we find the magnetic catalysis of chiral symmetry breaking; on the other hand, the electric field has the opposite effect, leading to an inverse magnetic catalysis [51]. In this pure electric field case, there exists a critical electric field at which chiral symmetry is restored in the chiral limit: We find the transition to be of the second order. In the case of massive quarks, the phase transition is changed into a smooth crossover characterized by a smooth but net change in the slope of the condensate, resulting in a smaller value of the condensate itself, as happens for the chiral phase transition at a finite temperature. In this case, it is not possible to define in a rigorous way a critical field, but it is still possible to identify a range of electric fields in which M_q has its highest change with E and identify this range with the pseudocritical region.

It is interesting to study what happens when E and B act together: Naturally, one would expect a competition among the effects of the magnetic (catalysis) and electric (inverse catalysis) fields. In Fig. 1, we have shown the case $E = B$ in which it is clear that, regardless of whether we work in the chiral or in the physical current quark mass limit, the magnetic field has some catalysis effect increasing the value of M_q (i.e., chiral condensate) and shifts the critical (or pseudocritical) value of the electric field slightly upwards compared to the case $B = 0$. In Fig. 2, we show M_q as a function of eB for several choices of E, starting from $E = 0$ up to $E = B$. Already for $E = 0.5B$ we find a sign of competition among direct and inverse catalysis, which manifests in a nonmonotonic behavior of M_q versus eB. We can also read the results of Fig. 2 in the opposite way:

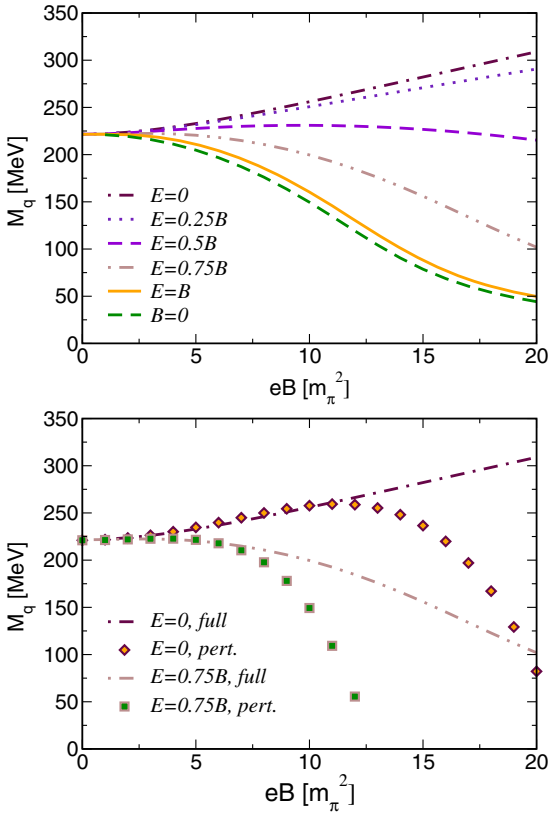

FIG. 2. Upper panel: Dynamical quark mass versus the magnetic field strength at zero temperature, for several values of the background electric field. The maroon dot-dashed line corresponds to the case of a pure magnetic field; the indigo dotted line to $E = 0.25B$; the dashed magenta line to $E = 0.5B$; the dot-dot-dashed brown line to $E = 0.75B$; and, finally, the orange line to $E = B$. For comparison, we have also shown data for $B = 0$ borrowed from Fig. 1; in this case, on the x axis we show eE in units of m_π^2. Lower panel: Comparison of the perturbative solution Eq. (7) with the full one.

Given a background of an electric field E, even introducing a magnetic field of the same magnitude of E does not result in a considerable change of spontaneous chiral symmetry breaking—compare the green dashed and orange solid lines in Fig. 1; for B as large as $\approx 1.3E$, we find that qualitatively the behavior of the chiral condensate versus field strength is like the one at $B = 0$, even if for very small values of the field strength we still find the mass increases; the net effect of the magnetic field is to shift the critical value of the electric field to larger values because of catalysis. In order to measure a catalysis effect, one has to introduce a larger magnetic field, for example, $B \approx 2E$ in Fig. 2. The inverse catalysis effect induced by the electric field and the second electromagnetic invariant $\boldsymbol{E} \cdot \boldsymbol{B}$ are in agreement with previous studies at zero temperature [37–41].

The behavior of M_q for small values of the fields can be easily understood quantitatively by the gap equation at $T = 0$ and $m_0 = 0$. We can find an analytical solution for the gap equation (4) for small fields by writing $M_q = M_0 + \delta m$,

where M_0 corresponds to the solution of the gap equation for $E = B = 0$. Moreover, for small values of the fields we can keep only the order $O(M_0)$ in the field-dependent term in Eq. (4). Taking into account that M_0 is the solution of the gap equation at $E = B = 0$, we find

$$\delta m = \frac{1}{2N_f |E_i(-M_0^2/\Lambda^2)|}(\Upsilon_1 + \Upsilon_2), \tag{7}$$

where

$$\Upsilon_1 = \frac{q_u^2 + q_d^2}{3M_0^3}\mathcal{I}_1, \tag{8}$$

$$\Upsilon_2 = -\frac{q_u^4 + q_d^4}{45M_0^7}(\mathcal{I}_1^2 + 7\mathcal{I}_2^2), \tag{9}$$

with $\mathcal{I}_1 \equiv (eB)^2 - (eE)^2$ and $\mathcal{I}_2 \equiv (eE)(eB)$; moreover, E_i denotes the exponential integral function $E_i(x) = -\int_{-x}^{\infty} ds e^{-s}/s$. The field dependence in the above equation resembles that occurring in the Euler-Heisenberg Lagrangian [54] as it should, since the latter can be obtained by integrating the gap equation over M_q. From Eq. (7), we notice that, for $B = 0$, $\delta m \propto -E^2/M_0^3$ neglecting higher-order contributions; the curvature of δm versus eE does not change as long as $eE > eB$. For $E = B$, one has to take into account the contribution $O(E^2B^2)$, which still shows $\delta m \propto -E^2B^2/M_0^7$ leading to a decreasing M_q. Finally, for $eB > eE$, the catalysis sets in, at least for small values of the fields, eventually leading to $\delta m \propto -B^2/M_0^3$ for $E = 0$. In the lower panel in Fig. 2, we have compared the perturbative solution in Eq. (7) with the full one, for two cases. We find a fair agreement among the two for eE, $eB \simeq 5m_\pi^2$.

IV. RESULTS AT A FINITE TEMPERATURE

In this section, we discuss our results about chiral symmetry restoration at a finite temperature. In the upper panel in Fig. 3, we plot M_q versus T for $E \neq 0$ and $B \neq 0$ and compare it with the result at $E = B = 0$. The general trend of data shown in the figure is in agreement with the scenario depicted at $T = 0$ discussed above. In particular, the inverse catalysis due to the electric field implies the lowering of the critical temperature; on the other hand, the catalysis due to the magnetic field at $T = 0$ is still present at $T \approx T_c$, leading to the increase of the pseudocritical temperature at $B \neq 0$. It has been discussed that the magnetic catalysis of chiral symmetry breaking within the NJL model at a finite temperature is due to the fact the NJL interaction kernel does not take into account the effects of screening as well as of coupling lowering which instead occur in QCD and are important for inverse catalysis [55,56]. Although it would be possible to insert by hand a B dependence of the NJL coupling in order to reproduce the inverse magnetic catalysis [57], we prefer to not do this in our study, because it would hide the effect of the electric field; we will add this important ingredient in our upcoming works.

In the middle panel in Fig. 3, we plot $|dM_q/dT|$: We identify its maximum with the crossover temperature. For $E = B = 0$, we find $T_c \approx 166$ MeV. We notice that the electric field not only makes the pseudocritical temperature

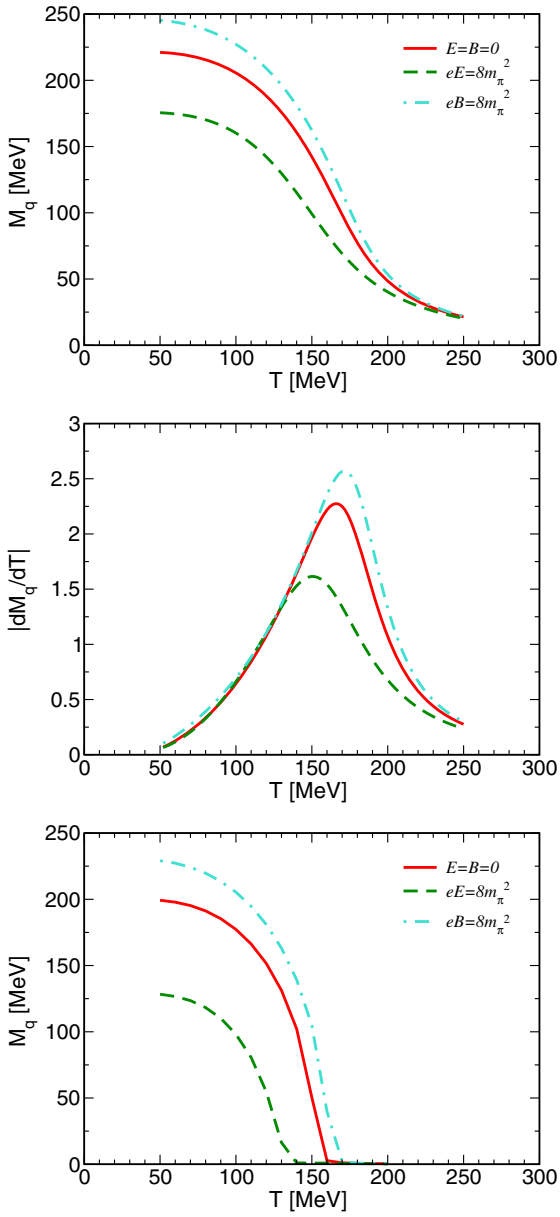

FIG. 3. Upper panel: Dynamical quark mass versus the temperature for $E = B = 0$ (red solid line), $eB = 8m_\pi^2$ (cyan dot-dashed line), and $eE = 8m_\pi^2$ (dashed green line). Middle panel: $|dM_q/dT|$ versus the temperature used to identify the pseudocritical temperature for the chiral crossover. The line convention is the same as the upper panel. Lower panel: Dynamical quark mass versus the temperature for $E = B = 0$ (red solid line), $eB = 8m_\pi^2$ (cyan dot-dashed line), and $eE = 8m_\pi^2$ (dashed green line) in the chiral limit.

lower than the one in the case $E = B = 0$, but it also smooths the crossover because the variation of the quark mass with the temperature is smaller in magnitude than in the case with no fields. Finally, in the lower panel in Fig. 3, we plot M_q versus the temperature for the ideal case of quarks with vanishing current mass: As expected, the effect of the external fields is qualitatively the same we have found in the realistic case of quarks with finite current mass.

In Fig. 4, we plot M_q versus T for several values of E and B: Thin lines correspond $B = 0$, while with thick lines we denote the results for $E = B$. The blue solid line corresponds to $eE = m_\pi^2$, the orange dotted line to $eE = 8m_\pi^2$, and the green dashed line to $eE = 15m_\pi^2$. Increasing the electric field strength results in a lowering of the critical temperature, and the effect of $B \neq 0$ is just to increase a bit the quark mass and shift the critical temperature towards slightly higher values.

The results collected in Figs. 3 and 4 show that even when $B = E$ the effect of the fields on the critical temperature does not cancel and the electric field gives the more important contribution, leading to an inverse catalysis. In fact, one would need a larger value of B to observe an increase of the critical temperature. This can be understood easily: Close to the second-order phase transition (we work now at $m_0 = 0$, which allows an analytical treatment), we can make an expansion of the thermodynamic potential in powers of M_q, namely,

$$\Omega = \frac{\alpha_2}{2} M_q^2 + O(M_q^4), \tag{10}$$

where the coefficient $\alpha_2 = \partial^2\Omega/\partial M_q^2$ at $M_q = 0$; α_2 is negative in the chirally broken phase and vanishes at the phase transition. The coefficient α_2 can be easily computed taking the derivative of the gap equation [Eq. (4)] and

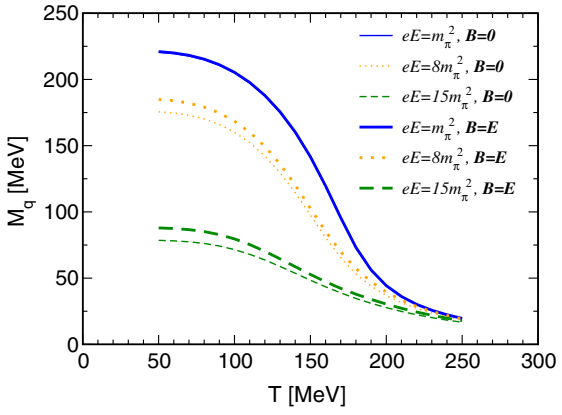

FIG. 4. Dynamical quark mass versus the temperature for several values of E and B. Thin lines correspond $B = 0$, while with thick lines we denote the results for $E = B$. The blue solid line corresponds to $eE = m_\pi^2$, the orange dotted line to $eE = 8m_\pi^2$, and the green dashed line to $eE = 15m_\pi^2$. The color convention for thick lines follows that we have used for thin lines.

expanding for small values of the fields. It is then possible to write $\alpha_2 = \alpha_{2,0} + \alpha_{2,2}$, where $\alpha_{2,0}$ denotes a field-independent term and $\alpha_{2,2}$ corresponds to a term $O(eE^2, eB^2)$. The field-independent term is not interesting, because it just determines the critical temperature when the external fields are set to zero. On the other hand, the field-dependent contributions are more relevant for the discussion; a straightforward calculation leads to

$$\alpha_{2,2} = -\sum_f q_f^2 \frac{N_c}{4\pi^2} \int ds \Theta_3(T,s) \frac{(eB)^2 - (eE)^2}{3} - \sum_f q_f^2 \frac{N_c}{48\pi^2 T^2} \int \frac{ds}{s} e^{-\frac{1}{4T^2 s}} \Delta_3(T,s)(eE)^2, \tag{11}$$

where we have used the shorthand notation

$$\Theta_3(T,s) = \theta_3\left(\frac{\pi}{2}, e^{-\frac{1}{4T^2 s}}\right), \tag{12}$$

$$\Delta_3(T,s) = \left.\frac{d\theta_3(z,x)}{dx}\right|_{z=\frac{\pi}{2}, x=\exp[-1/(4T^2 s)]}. \tag{13}$$

The term on the right-hand side in the first line of Eq. (11) shows that the correction to α_2 due to the pure magnetic field is negative, hence shifting the phase transition to larger temperatures. On the other hand, the term proportional to E^2 is positive and gets a further positive contribution from the second line of Eq. (11): Indeed, the latter is proportional to the derivative of the $\theta_3(x,z)$ function, which is a decreasing function of its second argument. As a consequence, the coefficient proportional to E^2 is positive, and, because of the additional contribution at a finite temperature, one needs a value of $B > E$ in order to change the sign of $\alpha_{2,2}$ and turn the inverse catalysis into a direct one. This explains why for $E = B$ we still find an inverse catalysis of chiral symmetry breaking at a finite temperature.

In Fig. 5, we plot T_c versus eE (measured in units of m_π^2) for several values of the external magnetic field: Black

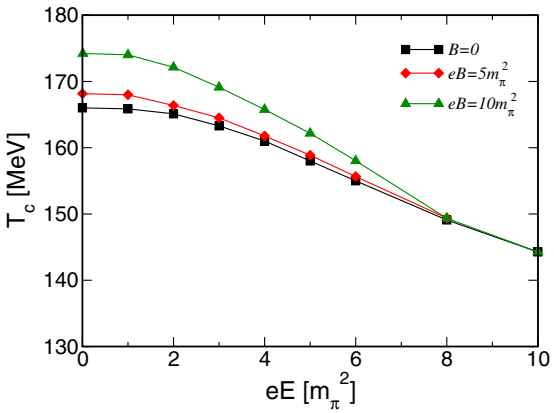

FIG. 5. Critical temperature for chiral symmetry restoration versus electric field strength, measured in units of m_π^2, for several values of the external magnetic field.

squares correspond to $B = 0$, red diamonds to $eB = 5m_\pi^2$, and green triangles to $eB = 10m_\pi^2$. This figure summarizes one of the main findings of our work, namely, that the electric field leads to a lowering of the critical temperature for chiral symmetry restoration, and the presence of the parallel magnetic field does not change this result unless $B \gg E$.

V. CHIRAL DENSITY EFFECTS AT THE CRITICAL TEMPERATURE

The electric-magnetic background considered in this article is dynamically unstable because of the Schwinger pair production [53,54]. This is due to the presence of poles in the thermodynamic potential Ω, which in turn make the quantum corrections to the electromagnetic Lagrangian complex, with the imaginary part related to the vacuum persistency probability. Because of the quantum anomaly, the Schwinger mechanism eventually leads to a nonzero chiral density n_5; we assume for the moment that the background magnetic field B is very large, so that it is reasonable to assume that only the LLL is occupied, to simplify the discussion; moreover, we assume the system to be made only of one flavor of quarks, namely, u quarks. Let us focus on one single $u\bar{u}$ created by the Schwinger effect. The u quark must have its spin aligned along $\boldsymbol{B}$ because of the LLL approximation; because of dimensional reduction in the LLL, u momentum will be initially rather parallel or antiparallel to $\boldsymbol{B}$, so the initial chirality can be either positive or negative. On the other hand, the effect of $\boldsymbol{E}\|\boldsymbol{B}$ is to accelerate u along the direction of $\boldsymbol{B}$ so after some time u quark will have positive chirality. An analogous discussion can be done for the $\bar{u}$. Therefore, as a consequence of the Schwinger effect, LLL, and $\boldsymbol{E}\|\boldsymbol{B}$ each time a pair is created, there is an increase of a factor of 2 of the net chiral density of the system, $n_5 \equiv n_R - n_L$. Obviously, higher Landau levels do not contribute to n_5, because particle spin can be either parallel or antiparallel to $\boldsymbol{B}$, leading to a cancellation of n_5. Hence, chirality is produced dynamically in the background field configuration studied here. This makes the study very interesting, because if chiral density relaxes to an equilibrium value, it might affect the equilibrium properties of quark matter.

The time evolution of n_5 in the case of massive particles in the background with constant and homogeneous fields has been derived for the first time by Warringa in [48], where he has shown it can be directly obtained from the Schwinger production rate for the case of $\boldsymbol{E}\|\boldsymbol{B}$, namely [58–62],

$$\Gamma = \frac{q_f^2(eE)(eB)}{4\pi^2}\coth\left(\frac{B}{E}\right)e^{-\frac{\pi M^2}{|q_f eE|}}; \tag{14}$$

indeed, only the LLL gives a contribution to n_5, and this LLL contribution can be easily extracted from the above equation by taking the $B \to \infty$ limit, because in such a limit it is reasonable to assume that only the LLL is occupied; because each pair in the LLL changes the chiral density of a factor of 2, we have from the above equation in the $B \to \infty$ limit

$$\frac{dn_5}{dt} = \frac{q_f^2(eE)(eB)}{2\pi^2}e^{-\frac{\pi M^2}{|q_f eE|}}, \tag{15}$$

in agreement with Ref. [48]. If evolution of n_5 was given only by the above equation, then the system would never be able to reach thermodynamical equilibrium (assuming the fields as external fields neglecting any backreaction from the fermion currents). However, Eq. (15) is just half of the story: Because of the finite quark mass, there are chirality-changing processes which should lead to the equilibration of n_5. In order to take into account these processes, we add a relaxation term on the right-hand side of the above equation:

$$\frac{dn_5}{dt} = \frac{q_f^2(eE)(eB)}{2\pi^2}e^{-\frac{\pi M^2}{|q_f eE|}} - \frac{n_5}{\tau_M}, \tag{16}$$

where τ_M corresponds to the relaxation time of chirality-changing processes. For $t \gg \tau_M$, the solution of Eq. (16) relaxes to the equilibrium value

$$n_5^{\mathrm{eq}} = \frac{q_f^2(eE)(eB)}{2\pi^2}e^{-\frac{\pi M^2}{|q_f eE|}}\tau_M. \tag{17}$$

The equilibrium value of the chiral density depends on the value of τ_M. It is reasonable to assume both by virtue of dimensional considerations and by naive physical arguments that $\tau_M \propto 1/M_q$, where M_q corresponds to the constituent quark mass: For large values of M_q, chirality-changing processes will be very fast, hence reducing drastically the relaxation time and the net chirality produced at equilibrium; on the other hand, for small M_q, the system will be less efficient in changing chirality, which implies a larger relaxation time and a larger chirality produced at equilibrium. Thus, we assume

$$\tau_M = \frac{c}{M_q}; \tag{18}$$

the above equation implicitly contains effects of the chiral condensate in the chirally broken phase via the larger value of M_q in this phase. Needless to say, the parameter c adds the largest uncertainty in our calculations: Because n_5^{eq} depends linearly on τ_M, a change of an order of magnitude in c will produce the same change in n_5^{eq}. We will study how changing c might affect our results.

Equation (17) shows that on a time scale larger than the relaxation time an equilibrium value of n_5, namely, n_5^{eq}, is produced. Because of the different charges of u and d

quarks, the equilibrium value of n_5 for the two flavors to be different at equilibrium, in fact, we find

$$\frac{n_{5u}^{\rm eq}}{n_{5d}^{\rm eq}} = \frac{q_u^2}{q_d^2} e^{-\frac{\pi M^2}{|eE|}\left(\frac{1}{q_u}-\frac{1}{|q_d|}\right)}, \tag{19}$$

the actual value depending on E and on the temperature via M_q. The existence of an equilibrium value for the chiral density means it is possible to introduce a chemical potential for the chiral charge, namely, the chiral chemical potential μ_5, conjugated to $n_5^{\rm eq}$. A self-consistent computation of μ_5 given the value of $n_5^{\rm eq}$ in Eq. (17) requires a canonical ensemble calculation in which the gap equation for the quark mass is solved self-consistently with the number equation, namely,

$$n_5^{\rm eq} = -\frac{\partial\Omega}{\partial\mu_5}, \tag{20}$$

with μ_5 introduced in the quark propagator with $\boldsymbol{E}\|\boldsymbol{B}$. This full calculation is well beyond the purpose of the present article and is left to a future study. Here we limit ourselves to consider this problem only in the limit of small μ_5 as well as small fields, in which we can use the NJL model with $E = B = 0$ but $\mu_5 \neq 0$ to compute the relation between μ_5 and $n_5^{\rm eq}$, as well as to take into account self-consistently the effect of μ_5 in the gap equation. The cheap procedure we use here to solve the problem self-consistently should be accurate up to the lowest nontrivial order in μ_5 and fields, that is, $O(\mu_5^2, E^2, B^2)$.

The NJL thermodynamic potential at $E = B = 0$ and $\mu_5 \neq 0$ can be written as [26]

$$\Omega = \frac{(M_q - m_0)^2}{4G} - N_c \sum_f T \sum_n \int \frac{d^3\boldsymbol{p}}{(2\pi)^3} \log(\omega_n^2 + E_+^2)(\omega_n^2 + E_-^2), \tag{21}$$

with $E_\pm^2 = (p \pm \mu_{5f})^2 + M_q^2$ and μ_{5f} denotes the chiral chemical potential for the flavor f: We allow for a flavor dependence of μ_5, because the equilibrium value of n_5 depends on the flavor itself. At lowest order in μ_5 the correction to the thermodynamic potential can be written as

$$\delta\Omega = -N_c \sum_f \mu_{5f}^2 T \sum_n \int \frac{d^3\boldsymbol{p}}{(2\pi)^3} \frac{2(\omega_n^2 + M_q^2 - p^2)}{(p^2 + \omega_n^2 + M_q^2)^2}, \tag{22}$$

which allows one to write the μ_5-dependent correction to the gap equation, namely,

$$\frac{\partial\delta\Omega}{\partial M_q} = -N_c \sum_f \mu_{5f}^2 T \sum_n \int \frac{d^3\boldsymbol{p}}{(2\pi)^3} \frac{4M_q(3p^2 - \omega_n^2 - M_q^2)}{(p^2 + \omega_n^2 + M_q^2)^3}. \tag{23}$$

Moreover, the relation among $n_5 = -\partial\Omega/\partial\mu_5$ and μ_5 is given by

$$n_{5f} = \mu_{5f} N_c T \sum_n \int \frac{d^3\boldsymbol{p}}{(2\pi)^3} \frac{4(\omega_n^2 - p^2 + M_q^2)}{(p^2 + \omega_n^2 + M_q^2)^2}, \tag{24}$$

and the number equation [Eq. (20)] can be written as

$$n_{5f} = n_5^{\rm eq}. \tag{25}$$

We have verified that in the chiral limit $M_q = 0$ the above equation gives $n_{5f} = \mu_5 T^2 N_c/3$ in agreement with Ref. [6]; in the case $M_q \neq 0$, the relation between n_5 and μ_5 is more complicated, and we have to compute it by performing numerically the integration in Eq. (24).

Taking into account Eq. (23), the gap equation [Eq. (4)] becomes

$$\frac{M_q - m_0}{2G} = M_q \frac{N_c}{4\pi^2} \sum_f \int_0^\infty \frac{ds}{s^2} e^{-M_q^2 s} \mathcal{F}(s) + M_q \frac{N_c N_f}{4\pi^2} \int_{1/\Lambda^2}^\infty \frac{ds}{s^2} e^{-M_q^2 s} - \frac{\partial\delta\Omega}{\partial M_q}, \tag{26}$$

and μ_5 has to be computed self-consistently according to the number equation [Eq. (25)]. We notice that, although an explicit dependence of μ_5 on E and B is not present in the above equations, the gap equation [Eq. (24)] is coupled because of the dependence of $n_5^{\rm eq}$ on the M_q.

In Fig. 6, we plot M_q versus the temperature for several cases: The maroon solid line corresponds to $E = B = 0$ and $\mu_5 = 0$. The indigo dashed line corresponds to $E = B = 0$ and a common value $\mu_5 = 200$ MeV for u and d quarks: We plot these data to show that the NJL model we use in the calculation is capable of capturing the catalysis of chiral symmetry breaking at finite μ_5 since both M_q and T_c are shifted towards higher values in comparison with the case $\mu_5 = 0$. The orange dotted line corresponds to the case $E = B = 8m_\pi^2$ and $\mu_5 = 0$: These data are the same we have shown in Fig. 4. Finally, the green dot-dashed line corresponds to $E = B = 8m_\pi^2$, with both M_q and μ_5 computed self-consistently by solving the number equation [Eq. (25)] and the gap equation [Eq. (23)] simultaneously. Although $eE = 8m_\pi^2$ sounds large for the approximation to be reliable, we present this result first because it magnifies the effect of the self-consistent μ_5 which would be otherwise not easy to see. In the lower panel in Fig. 6, we plot the chiral chemical potential for u (thick dot-dashed line) and d (thin dot-dashed line) quarks versus the temperature,

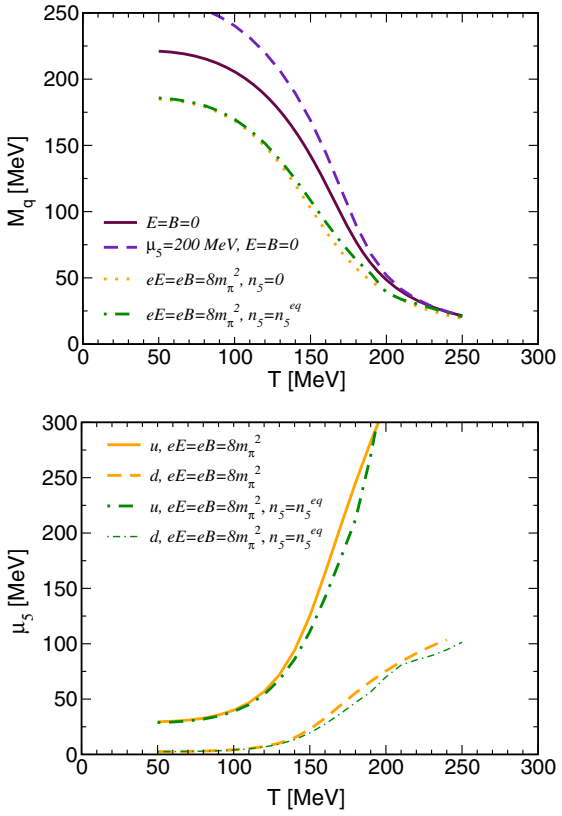

FIG. 6. Upper panel: M_q versus the temperature. The maroon solid line corresponds to $E = B = 0$ and $\mu_5 = 0$. The indigo dashed line corresponds to $E = B = 0$ and $\mu_5 = 200$ MeV for u and d quarks. The orange dotted line corresponds to the case $E = B = 8m_\pi^2$ and $\mu_5 = 0$: These data are the same we have shown in Fig. 4. The green dot-dashed line corresponds to $E = B = 8m_\pi^2$, with both M_q and μ_5 computed self-consistently by the condition $n_5 = n_5^{\rm eq}$ with n_5 given by Eq. (24) and the gap equation [Eq. (23)]. Lower panel: Self-consistent μ_5 (green lines) for u (thick dot-dashed line) and d (thin dot-dashed line) quarks versus the temperature, corresponding to M_q shown in the upper panel. For comparison, we have also shown the chiral chemical potential obtained by M_q computed with $\mu_5 = 0$ shown in the upper panel.

corresponding to M_q shown in the upper panel. For comparison, we have also shown the chiral chemical potential obtained by M_q computed with $\mu_5 = 0$ shown in the upper panel. Comparing the results obtained with $\mu_5 = 0$ and self-consistent μ_5, we notice a slight back-reaction of the equilibrium chiral density on the quark condensate, which reflects in a small change of M_q; moreover, the catalysis induced by μ_5 is observed thanks to a slight shift of the inflection point of M_q towards a larger temperature. However, still the combined effect of n_5 at equilibrium and $\boldsymbol{E}\|\boldsymbol{B}$ is to lower T_c with respect to the case $E = B = 0$.

We have verified that this scenario is in qualitative agreement with the one obtained for smaller values of E and B, in which case our approximation should be quantitatively more reliable. In the upper panel in Fig. 7, we plot M_q versus the temperature for $E = B = 8m_\pi^2$ (orange lines) and $E = B = 3m_\pi^2$ (green lines), as well as for the case $E = B = 0$, which we use as a benchmark (solid maroon line). In the lower panel in Fig. 7, we plot the chiral chemical potentials for u and d quarks at equilibrium computed self-consistently. We find no qualitative difference between the cases of small and large fields.

For completeness, we report the average value of n_5 in the crossover region, namely, in the temperature range (150–200) MeV, which can be obtained directly by using Eq. (17). We find it runs in the range 0.015–0.16 fm^{-3} in the case of $E = B = 3m_\pi^2$ and 0.25–1.10 fm^{-3} in the case of $E = B = 8m_\pi^2$.

The reason why M_q is poorly affected by μ_5 for small values of the fields is the different relative change of critical temperature induced by μ_5, on the one hand, and the electric field, on the other hand. In the case $eE = eB = 3m_\pi^2$ in Fig. 7, the average values of μ_5 are less than 10 MeV in the crossover region. By taking $\mu_5 = 0$, the effect of E and B is to lower the critical temperature by about 5%; on the other hand, by taking $E = B = 0$ and $\mu_5 = 10$ MeV, the shift of T_c is practically zero. Even by increasing by hand the value of μ_5 of a factor of 10, the increase of T_c due to μ_5 is practically negligible compared to the lowering induced by the fields.

The results shown in Fig. 7 have been obtained for $c = 1$ in Eq. (18). We have checked the stability of the results in the case $eE = 3m_\pi^2$ by increasing the relaxation time by an order of magnitude: We collect the results of this check in Fig. 8. In the upper panel in Fig. 8, we plot M_q versus the temperature in the pseudocritical region. Maroon and green lines represent the same quantities as in Fig. 7; indigo stars correspond to M_q computed with $\tau_M = 10/M_q$ in Eq. (17), and a turquoise plus denotes the solution of the gap equation for a fixed value of $\mu_5 = 75$ MeV. We find that for large temperatures the effect of the larger relaxation appears as a tiny shift of M_q towards larger values; this can be understood because the values of μ_{5u}, μ_{5d} in this case are larger than those found with $c = 1$; see the lower panel in Fig. 8. However, still the average value of the chiral chemical potentials is quite small in the pseudocritical region. For comparison, we have shown the results of a computation at fixed value of $\mu_5 = 75$ MeV in the figure: This value of the chemical potential approximately corresponds to the average value $(\mu_{5u} + \mu_{5d})/2$ computed self-consistently in the case $\tau_M = 10/M_q$ at $T = 175$ MeV; see the indigo stars in the lower panel in Fig. 8. We find a fair agreement among the calculations with fixed and self-consistent μ_5, showing that the values of M_q we obtain in the self-consistent calculation are indeed those expected. We notice that in the case $\tau_M = 25/M_q$, shown in Fig. 8 by orange data, we measure a slightly larger increase of M_q

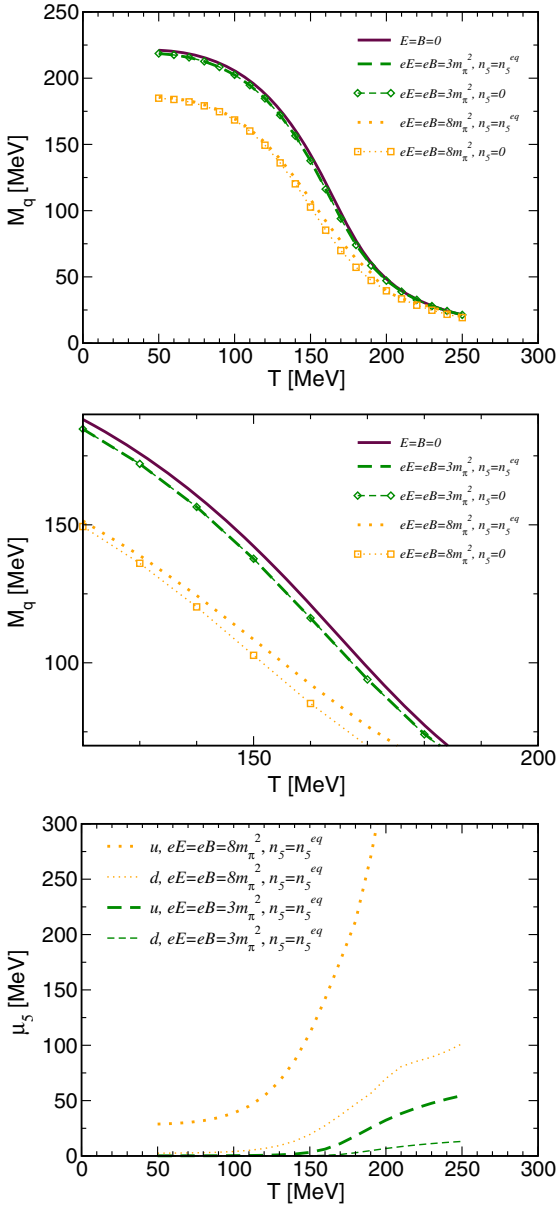

FIG. 7. Upper panel: M_q versus the temperature. The maroon solid line corresponds to $E = B = 0$ and $\mu_5 = 0$. The indigo dashed line corresponds to $E = B = 0$ and $\mu_5 = 200$ MeV for u and d quarks. The green lines correspond to $E = B = 8m_\pi^2$, the orange lines to $E = B = 8m_\pi^2$. Open symbols denote calculations at $\mu_5 = 0$, while thick lines are for results with μ_5 computed self-consistently by the number equation and the gap equation. Middle panel: Enlargement of the upper panel in the temperature range of the chiral crossover. Lower panel: Self-consistent μ_5 for u (thick lines) and d (thin lines) quarks versus the temperature, corresponding to M_q shown in the upper panel.

due to $\mu_5 \neq 0$ in the crossover region. This result clearly shows how a large μ_5 would affect the thermodynamics balancing the effect of the external fields; the concrete value of the average μ_5 we have in this case, however, runs in the range (40–320) MeV, so the result should not be trusted quantitatively.

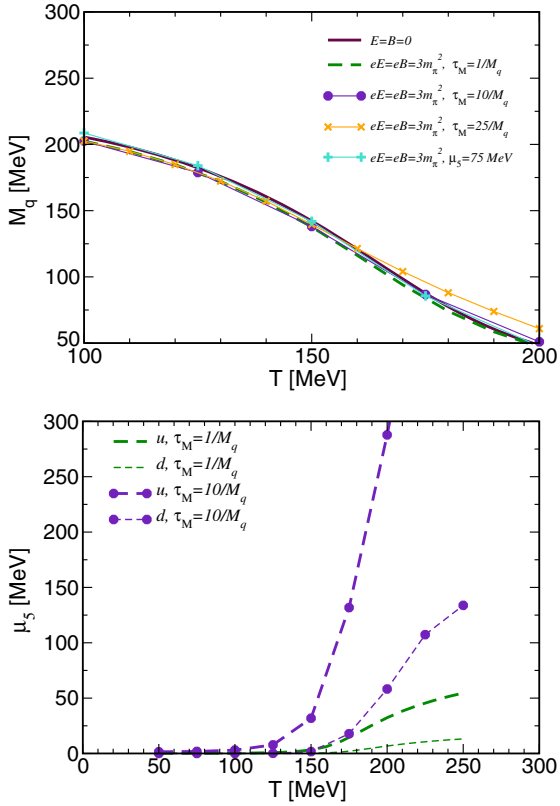

FIG. 8. Upper panel: M_q versus the temperature. The maroon solid line corresponds to $E = B = 0$ and $\mu_5 = 0$. The green line corresponds to $E = B = 3m_\pi^2$ with $\tau_M = 1/M_q$. The data represented by indigo stars denote M_q computed for $E = B = 3m_\pi^2$ with $\tau_M = 1/M_q$. The orange data correspond to $\tau_M = 25/M_q$. Finally, a turquoise plus corresponds to a calculation at a fixed value of $\mu_5 = 75$ MeV. Lower panel: Self-consistent μ_5 for u (thick lines) and d (thin lines) quarks versus the temperature, corresponding to M_q shown in the upper panel.

We have performed the stability check against variations of c or the case $E = B = 8m_\pi^2$ discussed above. We plot in Fig. 9 the result of this check for the cases of $\tau_M = 1/M_q$ (diamonds) and $\tau_M = 2/M_q$ (triangles). We have found that taking $c = 2$ affects M_q considerably, hence showing a net effect of chiral density on the phase transition. However, we take this result not too seriously, because doubling c would roughly correspond to doubling μ_5, which is already quite large in the pseudocritical region as it is shown in Fig. 7, hence making the use of our approximation questionable. Our conclusion is that, as long as the values of E and μ_5 are not too large, our approximate solution to the self-consistent problem is fairly good, while for larger values of the background field it has to be taken with a grain of salt.

In Fig. 10, we plot M_q versus the temperature for $eE = 3m_\pi^2$ and several values of eB. The computations have been performed by taking into account the dynamically generated n_5 for u and d quarks. It is interesting that, even if the magnetic field acts as a catalyzer of chiral symmetry

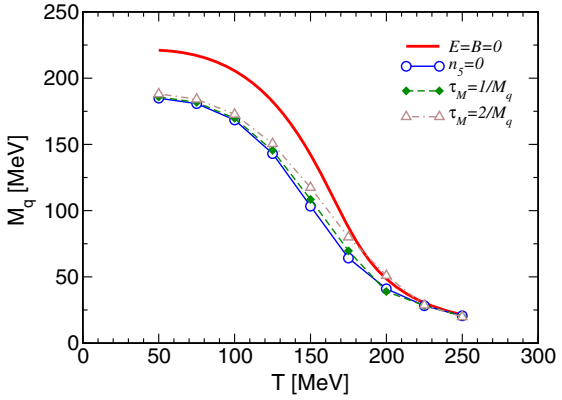

FIG. 9. M_q versus the temperature for $eE = eB = 8m_\pi^2$. As benchmarks we plot by a red solid line M_q for the zero field case and by circles M_q with $n_5 = 0$. Diamonds correspond to $\tau_M = 1/M_q$ and triangles to $\tau_M = 2/M_q$.

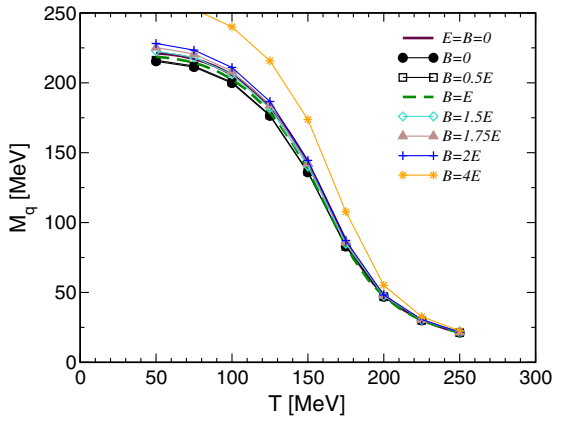

FIG. 10. M_q versus the temperature for $eE = 3m_\pi^2$ and several values of eB.

breaking at small temperatures, the presence of the electric field helps an inverse catalysis in the critical region: For example, in the case $B = 2E$ we find that M_q close to the critical temperature still sits on the zero field result; increasing the magnitude of E just moves the critical temperature to a lower value. This is in agreement with the analytical discussion in Sec. IV.

VI. CONCLUSIONS

In this article, we have studied spontaneous chiral symmetry breaking for quark matter in the background of static, homogeneous, and parallel electric field $\boldsymbol{E}$ and magnetic field $\boldsymbol{B}$. We have used a Nambu-Jona-Lasinio model with a local kernel interaction to compute the relevant quantities to describe chiral symmetry breaking at a finite temperature for a wide range of E and B.

Part of our study has been devoted to a mean field calculation of the response of the chiral condensate to the external fields, both at zero and at nonzero temperature. We have derived both numerically and analytically the magnetic catalysis and the electric inverse catalysis at zero temperature; we have also studied the behavior of the quark condensate at a finite temperature, finding a competition between the magnetic and electric fields which affects the critical temperature. We have not considered a by-hand modification of the NJL coupling constant in order to reproduce inverse magnetic catalysis for small B at a finite temperature, because this would have masked the genuine response of the model to an electric field, but we will certainly consider this necessary modification to the interaction term in the future. Our result in this direction is that the critical temperature for chiral symmetry restoration, T_c, is lowered by the simultaneous presence of the parallel electric and magnetic fields.

We have then focused on the effect of equilibration of the chiral density, n_5, produced dynamically by an axial anomaly on the critical temperature. A chiral density is produced thanks to Schwinger tunneling and spin alignment in the magnetic field. The equilibration of n_5 happens as a consequence of chirality-flipping processes in the thermal bath; we have introduced the relaxation time for chirality, namely, τ_M, giving the time scale necessary for the equilibration of n_5. In the absence of a specific calculation of τ_M, it is possible to give only an ansatz; we chose $\tau_M \propto 1/M_q$, where M_q is the constituent quark mass.

Because this dynamical system reaches a thermodynamical equilibrium state for $t \gg \tau_M$, with a specified value of $n_5 = n_5^{\mathrm{eq}}$ depending on the actual values of the field and of the temperature, it is possible to introduce the chiral chemical potential μ_5, conjugated to n_5^{eq} at equilibrium. The value of μ_5 has been computed by coupling the gap equation to the number equation, at the leading order in eE/T^2, eB/T^2, and μ_5/T. Because of the different electric charges of u and d quarks at equilibrium, $n_{5u}^{\mathrm{eq}} \neq n_{5d}^{\mathrm{eq}}$ and the ratio of the two is about 5:6 in the critical region; we have therefore introduced two chemical potentials μ_{5u} and μ_{5d} conjugated, respectively, to n_{5u}^{eq} and n_{5d}^{eq}.

We have found that the equilibrated chiral density does not change drastically the thermodynamics as long as μ_5 at equilibrium is not too large; namely, the inverse catalysis effect induced by the background fields is not spoiled by the presence of the μ_5 background. The weak effect of μ_5 on the shift of T_c in the presence of the background fields can be understood, because the change of T_c induced by μ_5 itself is smaller than the ones induced by the background fields. For example, in the case $\mu_5 = 0$, the effect of the background fields is to lower the critical temperature by about 5%; on the other hand, taking $E = B = 0$ and $\mu_5 = 10$ MeV, which corresponds to the average value of the chemical potential we find in the crossover region, the shift of T_c is practically zero. This conclusion might be no longer valid in the case of large μ_5. For larger values of the fields, we have found that M_q is effectively pushed towards larger values in the critical region by $\mu_5 \neq 0$. A firm conclusion about this finding can be achieved, however,

only by solving the problem beyond the perturbative analysis used in our study.

We remark that the results presented here have to be considered only explorative: The study of this problem beyond the weak field and small μ_5 approximation will be the topic of upcoming research. Moreover, the theoretical calculation of the equilibrium value of μ_5 has an uncertainty because of the lack of information about the relaxation time for chirality-flipping processes, τ_M in Eq. (18), whose computation will be the theme of near future research.

ACKNOWLEDGMENTS

The authors thank the CAS President's International Fellowship Initiative (Grant No. 2015PM008), and the NSFC Projects (No. 11135011 and No. 11575190).

[1] S. L. Adler, Phys. Rev. **177**, 2426 (1969).
[2] J. S. Bell and R. Jackiw, Nuovo Cimento A **60**, 47 (1969).
[3] G. D. Moore, arXiv:hep-ph/0009161.
[4] G. D. Moore and M. Tassler, J. High Energy Phys. 02 (2011) 105.
[5] D. E. Kharzeev, L. D. McLerran, and H. J. Warringa, Nucl. Phys. **A803**, 227 (2008).
[6] K. Fukushima, D. E. Kharzeev, and H. J. Warringa, Phys. Rev. D **78**, 074033 (2008).
[7] Q. Li *et al.*, arXiv:1412.6543.
[8] D. T. Son and P. Surowka, Phys. Rev. Lett. **103**, 191601 (2009).
[9] N. Banerjee, J. Bhattacharya, S. Bhattacharyya, S. Dutta, R. Loganayagam, and P. Surowka, J. High Energy Phys. 01 (2011) 094.
[10] K. Landsteiner, E. Megias, and F. Pena-Benitez, Phys. Rev. Lett. **107**, 021601 (2011).
[11] D. T. Son and A. R. Zhitnitsky, Phys. Rev. D **70**, 074018 (2004).
[12] M. A. Metlitski and A. R. Zhitnitsky, Phys. Rev. D **72**, 045011 (2005).
[13] D. E. Kharzeev and H. U. Yee, Phys. Rev. D **83**, 085007 (2011).
[14] M. N. Chernodub, J. High Energy Phys. 01 (2016) 100.
[15] M. N. Chernodub and M. Zubkov, arXiv:1508.03114.
[16] M. N. Chernodub, A. Cortijo, A. G. Grushin, K. Landsteiner, and M. A. H. Vozmediano, Phys. Rev. B **89**, 081407 (2014).
[17] V. Braguta, M. N. Chernodub, K. Landsteiner, M. I. Polikarpov, and M. V. Ulybyshev, Phys. Rev. D **88**, 071501 (2013).
[18] A. V. Sadofyev and M. V. Isachenkov, Phys. Lett. B **697**, 404 (2011).
[19] A. V. Sadofyev, V. I. Shevchenko, and V. I. Zakharov, Phys. Rev. D **83**, 105025 (2011).
[20] Z. V. Khaidukov, V. P. Kirilin, A. V. Sadofyev, and V. I. Zakharov, arXiv:1307.0138.
[21] V. P. Kirilin, A. V. Sadofyev, and V. I. Zakharov, arXiv:1312.0895.
[22] A. Avdoshkin, V. P. Kirilin, A. V. Sadofyev, and V. I. Zakharov, Phys. Lett. B **755**, 1 (2016).
[23] M. Ruggieri and G. X. Peng, arXiv:1602.03651.
[24] M. Ruggieri and G. X. Peng, arXiv:1602.05250.
[25] R. Gatto and M. Ruggieri, Phys. Rev. D **85**, 054013 (2012).
[26] K. Fukushima, M. Ruggieri, and R. Gatto, Phys. Rev. D **81**, 114031 (2010).
[27] M. N. Chernodub and A. S. Nedelin, Phys. Rev. D **83**, 105008 (2011).
[28] M. Ruggieri, Phys. Rev. D **84**, 014011 (2011).
[29] L. Yu, H. Liu, and M. Huang, arXiv:1511.03073.
[30] L. Yu, J. Van Doorsselaere, and M. Huang, Phys. Rev. D **91**, 074011 (2015).
[31] M. Frasca, arXiv:1602.04654.
[32] V. V. Braguta, E.-M. Ilgenfritz, A. Y. Kotov, B. Petersson, and S. A. Skinderev, Phys. Rev. D **93**, 034509 (2016).
[33] V. V. Braguta, V. A. Goy, E.-M. Ilgenfritz, A. Y. Kotov, A. V. Molochkov, M. Muller-Preussker, and B. Petersson, J. High Energy Phys. 06 (2015) 094.
[34] V. V. Braguta and A. Y. Kotov, arXiv:1601.04957 [Phys. Rev. D (to be published)].
[35] M. Hanada and N. Yamamoto, *Proc. Sci.*, LATTICE2011 (2011) 221 [arXiv:1111.3391].
[36] S. S. Xu, Z. F. Cui, B. Wang, Y. M. Shi, Y. C. Yang, and H. S. Zong, Phys. Rev. D **91**, 056003 (2015).
[37] A. Y. Babansky, E. V. Gorbar, and G. V. Shchepanyuk, Phys. Lett. B **419**, 272 (1998).
[38] S. P. Klevansky and R. H. Lemmer, Phys. Rev. D **39**, 3478 (1989).
[39] H. Suganuma and T. Tatsumi, Ann. Phys. (N.Y.) **208**, 470 (1991).
[40] K. G. Klimenko, Z. Phys. C **54**, 323 (1992).
[41] K. G. Klimenko, Teor. Mat. Fiz. **90**, 3 (1992) [Theor. Math. Phys. **90**, 1 (1992)].
[42] I. V. Krive and S. A. Naftulin, Phys. Rev. D **46**, 2737 (1992).
[43] V. P. Gusynin, V. A. Miransky, and I. A. Shovkovy, Phys. Rev. Lett. **73**, 3499 (1994); **76**, 1005(E) (1996).
[44] V. P. Gusynin, V. A. Miransky, and I. A. Shovkovy, Phys. Lett. B **349**, 477 (1995).
[45] G. Cao and X. G. Huang, Phys. Lett. B **757**, 1 (2016).
[46] M. D'Elia, M. Mariti, and F. Negro, Phys. Rev. Lett. **110**, 082002 (2013).
[47] G. Cao and X. G. Huang, Phys. Rev. D **93**, 016007 (2016).
[48] H. J. Warringa, Phys. Rev. D **86**, 085029 (2012).
[49] Y. Nambu and G. Jona-Lasinio, Phys. Rev. **122**, 345 (1961).
[50] Y. Nambu and G. Jona-Lasinio, Phys. Rev. **124**, 246 (1961).
[51] S. P. Klevansky, Rev. Mod. Phys. **64**, 649 (1992).
[52] T. Hatsuda and T. Kunihiro, Phys. Rep. **247**, 221 (1994).
[53] J. S. Schwinger, Phys. Rev. **82**, 664 (1951).

[54] W. Heisenberg and H. Euler, Z. Phys. **98**, 714 (1936). See also W. Korolevski and H. Kleinert, arXiv:physics/0605038 for an English translation.
[55] J. Braun, W. A. Mian, and S. Rechenberger, Phys. Lett. B **755**, 265 (2016).
[56] N. Mueller and J. M. Pawlowski, Phys. Rev. D **91**, 116010 (2015).
[57] A. Ahmad and A. Raya, arXiv:1602.06448.
[58] K. Fukushima, D. E. Kharzeev, and H. J. Warringa, Phys. Rev. Lett. **104**, 212001 (2010).
[59] A. I. Nikishov, Zh. Eksp. Teor. Fiz. **57**, 1210 (1969).
[60] T. D. Cohen and D. A. McGady, Phys. Rev. D **78**, 036008 (2008).
[61] F. V. Bunkin and I. I. Tugov, Dokl. Akad. Nauk Ser. Fiz. **187**, 541 (1969).
[62] G. V. Dunne, arXiv:hep-th/0406216.